



## Design, synthesis and antitumor activity of 4-aminoquinazoline derivatives targeting VEGFR-2 tyrosine kinase

Bing Yu<sup>a,b</sup>, Li-da Tang<sup>b,c</sup>, Yi-liang Li<sup>c</sup>, Shu-hui Song<sup>d</sup>, Xiao-liang Ji<sup>d</sup>, Mu-sen Lin<sup>d</sup>, Chun-Fu Wu<sup>a,\*</sup>

<sup>a</sup> Department of Pharmacology, Shenyang Pharmaceutical University, Shenyang 110016, People's Republic of China

<sup>b</sup> Research Center of New Drug Evaluation, Tianjin Institute of Pharmaceutical Research, Tianjin 300193, People's Republic of China

<sup>c</sup> Tianjin Key Laboratory of Molecular Drug & Drug Discovery, Tianjin Institute of Pharmaceutical Research, Tianjin 300193, People's Republic of China

<sup>d</sup> Tianjin University of Traditional Chinese Medicine, Tianjin, People's Republic of China

### ARTICLE INFO

#### Article history:

Received 3 August 2011

Revised 15 November 2011

Accepted 16 November 2011

Available online 23 November 2011

#### Keywords:

4-Aminoquinazolines

Synthesis

VEGFR-2

### ABSTRACT

We report herein the design and synthesis of novel 4-aminoquinazoline derivatives based on the inhibitors of VEGFR-2 tyrosine kinases. The VEGFR-2 inhibitory activities of these newly synthesized compounds were also evaluated and compared with that of ZD6474. We found that most of target compounds had good inhibitory potency. In particular, compounds **1h**, **1n** and **1o** were found to be 6, 2 and 2-fold more potent than the positive control ZD6474. The leading compound **1h** also showed an *in vivo* activity against HepG2 human tumor xenograft model in BALB/c-nu mice.

© 2011 Elsevier Ltd. All rights reserved.

Angiogenesis of tumor mass is the process of forming new blood vessels from existing ones of host, and is strictly controlled by the balance of a number of angiogenic positive factors and negative ones.<sup>1</sup> The break of the balance is thought to drive angiogenesis, which is involved in the expansion and metastasis of solid tumor.<sup>2</sup> The blockade of the tyrosine kinase VEGFR-2 signaling pathway may disrupt the angiogenesis process of solid tumor so that the developing tumor cells required blood flow grow slowly, even stop growth because of lack of nutrient and growth factors supported by freshly forming vessels.<sup>3</sup> Antiangiogenic therapy appears to have its

optimum efficacy if given daily or intermittently over a long time period.<sup>4</sup> It is directed mainly at proliferating capillary endothelial cells and does not cause bone marrow suppression, gastrointestinal symptoms or hair loss.<sup>5</sup> Antiangiogenic therapy has also been proposed as a potential strategy to avoid drug resistance as inhibitor of angiogenesis targets endothelial cells of blood capillaries, the progenitors of new blood vessels, which show relative genetic stability based on their normal complement of chromosome.<sup>6</sup> Angiogenesis inhibitors increase uptake of chemotherapeutic drugs in a tumor.<sup>7</sup> After the completion of chemotherapy, radiation or surgery,

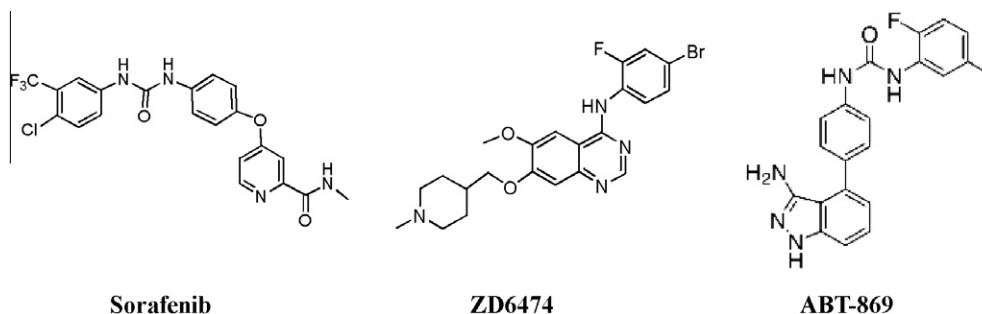
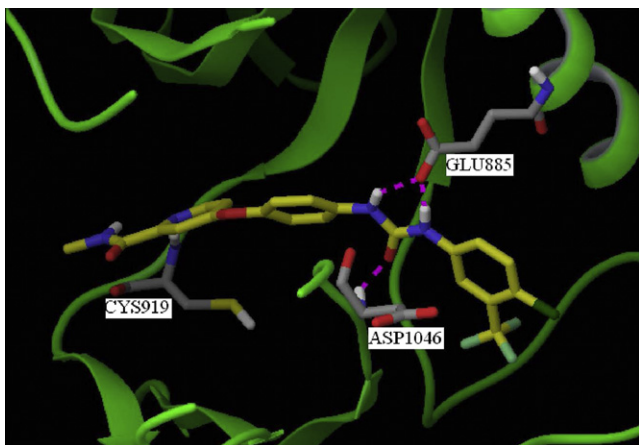


Figure 1. Examples of clinical VEGFR-2 kinase inhibitors.

\* Corresponding author. Tel./fax: +86 24 23843567.

E-mail address: [chunfuw@gmail.com](mailto:chunfuw@gmail.com) (C.-F. Wu).



**Figure 2.** Predicted binding mode of sorafenib in the X-ray structure of VEGFR-2 (PDB code 2RL5). Sorafenib (yellow carbon) was docked into the X-ray structure of VEGFR-2 using Glide method of Schrodinger software. Key hydrogen bond contacts are shown in dotted line.

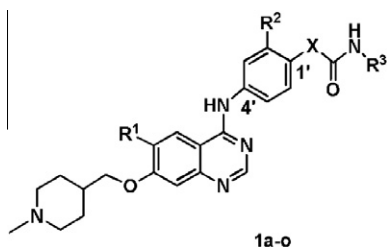


**Figure 3.** Structure of compounds **1a–o**.

antiangiogenic therapy may be continued for years because of its low toxicity, to prolong dormancy of microscopic metastases or to stabilize residual disease.<sup>8</sup>

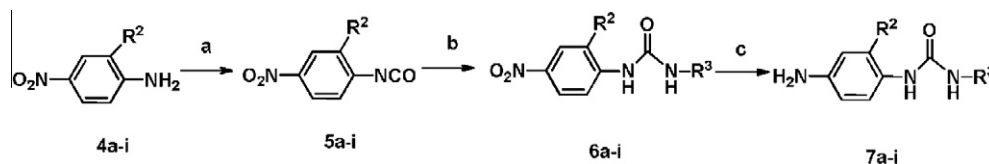
Recently, a number of VEGF receptor inhibitors have been reported. Sorafenib, marketed by Bayer and Onyx pharmaceuticals, has been shown to be a potent inhibitor of VEGF receptors *in vitro*. In

preclinical trials, sorafenib is shown to have broad spectrum antitumor activity in mouse models and is found to prevent the growth of tumors but not to reduce tumor size.<sup>9</sup> Sorafenib is approved by FDA for patients with metastatic renal cell carcinoma and hepatocellular carcinoma.<sup>10</sup> Although most of the VEGF receptor inhibitors currently on the market or under development are generally characterized by prominent anti-tumor growth effect, they also have respective shortage. For example, the water-solubility of Sorafenib and ABT-869 is not satisfactory,<sup>11</sup> while ZD6474 (Fig. 1) has good physico-chemical property but prolonging QT interval.<sup>12</sup>

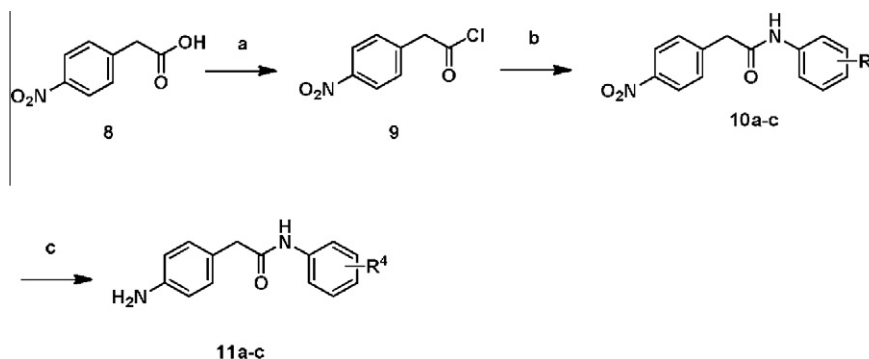
According to the structural analysis, both Sorafenib and ABT-869 contain aromatic urea fragment. The crystal structure of the complex between sorafenib and VEGFR-2 reveals that the urea portion occupies the back hydrophobic pocket with additional hydrogen-bonding interactions. When sorafenib is bound to VEGFR-2, it forms hydrogen bonds with the backbone-NH of Cys919, the side chain carboxylate of Glu885, and backbone-NH of Asp1046 (Fig. 2). The terminal phenyl moiety occupies the hydrophobic pocket created by rearrangement of the protein. Analysis of the X-ray structure also suggests sufficient space is available for the introduction of various substituents around the terminal benzene ring.

The introduction of carbamoylpyridyl increases the lipophilicity of the compounds ( $\log P = 5-6$ ). This increased lipophilicity is expected to decrease its water solubility of sorafenib. ZD6474 shows good water solubility, we reasoned that the basicity of the *N*-methylpiperidine ( $pK_a = 8.1$ ) improves the solubility of anilinoquinazolines. Based on the fragment drug design, we describe here the chemistry, SAR, and biological testing for these series. The quinazoline core was modified at position 4 of the aryl with different bulky substituents such as amide, carbamate or urea. These moieties appeared to be appropriate for modification in order to improve solubility as well as to enhance inhibitory potency against VEGFR-2. Based on the above hypothesis, we designed and synthesized the following compounds (**1**) (Fig. 3).

A general synthesis of aromatic urea and amide derivatives is shown in Schemes 1 and 2. Arylamines **4a–i** were treated with triphosgene at the presence of triethylamine to form isocyanates **5a–i**, which reacted with aniline derivatives followed by hydrolysis



**Scheme 1.** Synthesis of aromatic urea compounds **7a–i**. Reagents and conditions: (a) triphosgene,  $\text{CH}_2\text{Cl}_2$ , rt, triethylamine, 60–75%; (b)  $\text{CH}_2\text{Cl}_2$ , rt, 58–83%; (c) Pd/C, methanol, 80–86%.



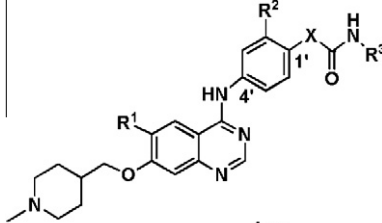
**Scheme 2.** Synthetic of aromatic amide compounds **11a–c**. Reagents and conditions: (a)  $\text{SOCl}_2$ , 60 °C, 86–93%; (b)  $\text{CH}_2\text{Cl}_2$ , rt,  $\text{K}_2\text{CO}_3$ , 90–95%; (c) Pd/C, methanol, 92–96%.

under basic conditions to provide the ureas **6a–i**. Using palladium-charcoal as the catalyst, reduction of **6a–i** performed smoothly in methanol to give **7a–i**. On the other hand, carboxylic acid **8** reacted with thionyl chloride to give acyl chloride **9**, which reacted with aniline derivatives to form amides **10a–c**. The nitro group of **10a–c** was reduced to amino group by Pd/C-catalyzed hydrogenation to give **11a–c**.

The synthesis of 4-substituted anilinoquinazolines derivatives compound **1a–o** was conducted as outlined in Scheme 3. Treatment of 7-fluoroquinazolone **12** with *N*-methyl-4-piperidinemethanol at the presence of NaH gave the corresponding C-7-piperidinemethoxyanilinoquinazolines derivatives **13**. 4-Chloroquinoline **14** was prepared by the chlorination of **13** with thionyl chloride, which was coupled with **7a–i** or **11a–c** to provide **1a–o**.<sup>13</sup>

These compounds were tested for VEGFR-2 kinase activity using homogeneous time resolved fluorescence (HTRF) method.<sup>14</sup> The catalytic activity of kinases was measured by phosphorylated biotin-peptide conjugate using streptavidin linked-APC and europium-labeled anti-phosphotyrosine antibody. Subsequently, a cell proliferation assay was performed to find the potent VEGFR-2 kinase inhibitors among these compounds for their ability to inhibit VEGF-stimulated proliferation of human umbilical vein endothelial cells (HUVEC).<sup>15</sup> The results are shown in Table 1. Overall, considerable relationships between their structures and inhibitory activities were observed. The urea compounds (X = NH) exhibited higher activity than the corresponding amides (X = CH<sub>2</sub>) as seen from **1g–i** versus **1a–c**, which demonstrated the importance of hydrogen bond between carbamido group and GLU885. Based on these findings, we further surveyed the effect of substitution at the nitrogen atom of carbamido group. Substitutions on the carbamido group in this study included ethyl, cyclopropyl, cyclohexyl and some kind of aryl group. As shown in Table 1, the activity imparted to the synthesized compounds by the R<sup>3</sup> was in the order of 3-F-Ph > 3-CF<sub>3</sub>-4-Cl-Ph ≈ 3-F-4-F-Ph > 3-Br-4-Me-Ph ≈ 2-F-4-Br-Ph > cyclopropyl > ethyl > cyclohexyl against VEGFR-2 and HUVEC-v cell. Because of the results that the 3-F-Ph group seemed to be optimal, we selected **1h** as the primer to carry out further research and focused on the halogenation on benzene ring of the side chain. There was a decrease in activity when a fluorine or chlorine atom was inducted at 2-position of the benzene ring as seen from **1l**, **1m** versus **1h**. On the other hand, **1h** and **1n** showed similar potency against VEGFR-2 while the latter compound was much less active against HUVEC-v cell. These results indicated that the C-6 methoxy group

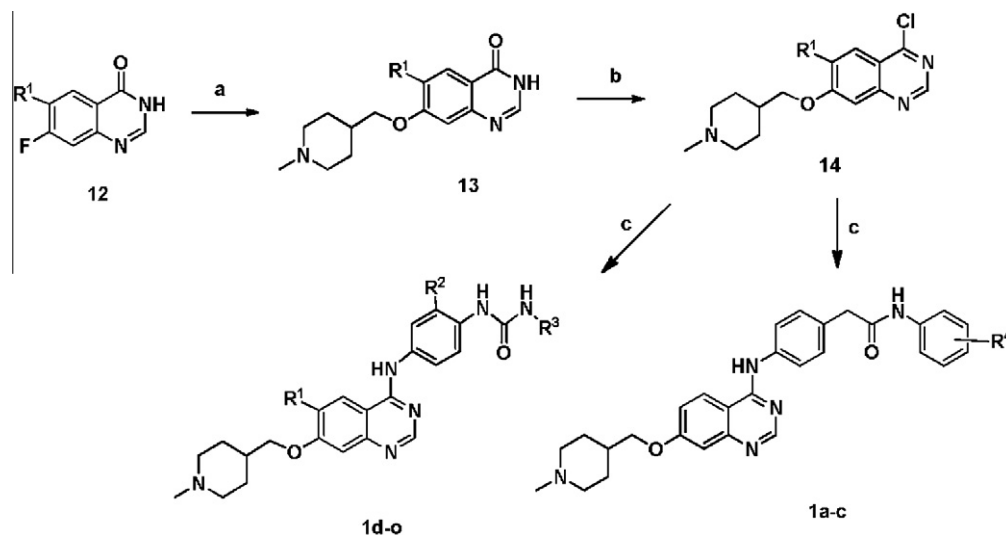
**Table 1**  
VEGFR-2 kinase and cell inhibitory activity compounds **1a–o**



Compound	X	R <sup>1</sup>	R <sup>2</sup>	R <sup>3</sup>	VEGFR-2 IC <sub>50</sub> (nM)	HUVEC-v IC <sub>50</sub> (nM)
<b>1a</b>	CH <sub>2</sub>	H	H	3-CF <sub>3</sub> -4-Cl-Ph	87	258
<b>1b</b>	CH <sub>2</sub>	H	H	3-F-Ph	65	237
<b>1c</b>	CH <sub>2</sub>	H	H	3-F-4-F-Ph	73	308
<b>1d</b>	NH	H	H	ethyl	105	587
<b>1e</b>	NH	H	H	cyclopropyl	98	324
<b>1f</b>	NH	H	H	cyclohexyl	237	—
<b>1g</b>	NH	H	H	3-CF <sub>3</sub> -4-Cl-Ph	23	92
<b>1h</b>	NH	H	H	3-F-Ph	5.5	52
<b>1i</b>	NH	H	H	3-F-4-F-Ph	25	89
<b>1j</b>	NH	H	H	4-CH <sub>3</sub> -3-Br-Ph	45	196
<b>1k</b>	NH	H	H	2-F-4-Br-Ph	50	233
<b>1l</b>	NH	H	F	3-F-Ph	15	67
<b>1m</b>	NH	H	Cl	3-F-Ph	17	132
<b>1n</b>	NH	OCH <sub>3</sub>	H	3-F-Ph	16	179
<b>1o</b>	NH	OCH <sub>3</sub>	F	3-F-Ph	17	185
ZD6474	—	—	—	—	35	187

of the quinazolinone ring played a negative role in drug entering the cell. This deduction was further supported by the fact that **1l** was two-fold more potent than **1o** against VEGFR-2, whereas it was almost opposite as to HUVEC-v cell. The reason for this is not clear, but the cellular permeability might influence the antiproliferative activity.

Table 2 shows the selective inhibitory potencies of compound **1h** against a panel of kinases. The compound **1h** is potent,



**Scheme 3.** Synthesis of compounds **1a–o**. Reagents and conditions: (a) NaH, DMF, 80 °C, 65–75%; (b) SOCl<sub>2</sub>, 60 °C, 75–83%; (c) isopropanol, 80 °C, 80–84%.

**Table 2**  
Kinase selectivity for compound **1h**

Kinase test	IC <sub>50</sub> (nM)
VEGFR-2	5.5
VEGFR-1	1920
VEGFR-3	9.6
PDGFR $\alpha$	1355
PDGFR $\beta$	2788
FGFR1	>10,000
Tie-2	>10,000
EGFR	>10,000
HER2	>10,000
AKT	8710
CDK1	10,000
Aurora A	2680

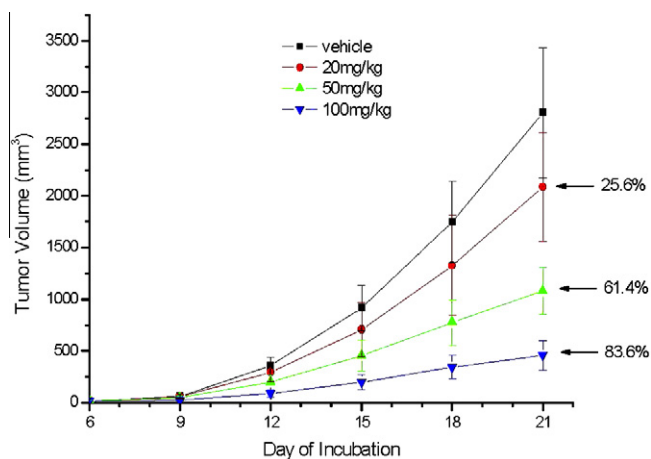


**Figure 4.** Effect of compound **1h** vehicle on tumor growth in xenograft model. HepG2 human hepatocarcinoma cells ( $1 \times 10^7$  cells) were implanted sc in the flank of BALB/c-nu mice. Five days after implantation following once daily oral administration of compound **1h** or vehicle. Data points represent mean  $\pm$  SE ( $n = 8$ ).

low-nanomolar inhibition of VEGFR-2, VEGFR-3. Other kinases such as VEGFR-1, PDGFR $\alpha$ , PDGFR $\beta$ , FGFR1, Tie-2, EGFR, HER2, AKT, CDK1 and AuroraA are only weakly inhibited.

Potential lead candidate compound **1h** was evaluated in vivo in the HepG2 cells, a human hepatocellular carcinoma cell line, as a xenograft model in BALB/c-nu mice. Following once daily oral administration of **1h** at three doses for 15 days, tumor growth inhibition (%TGI) of 25.6%, 61.4%, 83.6% was achieved at three doses of 20, 50, 100 mg/kg (Fig 4). No adverse events were observed. Oral administration **1h** was found to be well tolerated in the experiment, and the treated animals exhibited no clinically observable sign of toxicity or weight loss at the highest test dose of 100 mg/kg. It elicited robust and dose-proportional tumor responses over the dose range of 20–100 mg/kg in this tumor model.

In summary, we successfully developed a series of 4-anilinoquinazolines derivatives which showed potent, selective inhibition of the VEGFR-2 kinases. In the quinazoline series, compounds **1h**, **1n**, and **1o** displayed the most potent cytotoxic activity with IC<sub>50</sub> equal to 5.5, 16, and 17 nmol, respectively. The lead compound, **1h**, exhibited a good kinase selectivity, antiproliferative potency, oral exposure, and efficacy in tumor xenograft models. The further development of SAR was underway to find the more potent lead antitumor drug.

## Acknowledgments

The authors thank Dr. Meng, F. C. and Dr. He, H. W. for the molecular biology and in vivo assays. The work was supported

by the Nature Science Foundation of Tianjin, China (Grant ID No. 09JCZDJC21700).

## References and notes

- Carmeliet, P.; Jain, R. K. *Nature* **2000**, *407*, 249.
- (a) Folkman, J. *Semin. Oncol.* **2001**, *28*, 536; (b) Ferrara, N.; Gerber, H. P.; LeCouter, J. *Nat. Med.* **2003**, *9*, 669.
- (a) Peruzzi, B.; Bottaro, D. P. *Clin. Cancer Res.* **2006**, *12*, 3657; (b) Folkman, J. *Semin. Oncol.* **2002**, *29*, 15; (c) Ferrara, N. *Oncologist* **2004**, *9*, 2.
- (a) Kerbel, R. S. *BioEssays* **1991**, *13*, 31; (b) Crawford, J.; Ozer, H.; Stoller, R.; Johnson, D.; Lyman, G.; Tabbara, I.; Kris, M.; Grous, J.; Picozzi, V.; Rausch, G.; Smith, R.; Gradishar, W.; Yahanda, A.; Vincent, M.; Stewart, M.; Glaspay, J. N. *Engl. J. Med.* **1991**, *325*, 164.
- Wassberg, E.; Christofferson, R. *Eur. J. Cancer* **1997**, *33*, 2020.
- (a) Eikesdal, H. P.; Kalluri, R. *Semin. Cancer Biol.* **2009**, *19*, 310; (b) Azam, F.; Mehta, S.; Harris, A. L. *Eur. J. Cancer* **2010**, *46*, 1323.
- (a) Ma, J.; Waxman, D. J. *Clin. Cancer Res.* **2009**, *15*, 578; (b) Doloff, J. C.; Khan, N.; Ma, J.; Demidenko, E.; Swartz, H. M.; Jounaidi, Y. *Curr. Cancer Drug Targets* **2009**, *6*, 777.
- (a) Griffioen, A. W.; Barendsz-Janson, A. F.; Kevin, H. M.; Hillen, H. F. J. *Lab. Clin. Med.* **1998**, *132*, 363; (b) Kaban, K.; Herbst, R. S. *Hematol. Oncol. Clin. North Am.* **2002**, *16*, 1125.
- (a) Galle, P. R. J. *Hepatology* **2008**, *49*, 871; (b) Adnane, L.; Trail, P. A.; Taylor, I.; Wilhelm, S. M. *Methods Enzymol.* **2006**, *407*, 597; (c) Wilhelm, S. M.; Carter, C.; Tang, L.; Wilkie, D.; McNabola, A.; Rong, H.; Chen, C.; Zhang, X.; Vincent, P.; McHugh, M.; Cao, Y.; Shujath, J.; Gawlak, S.; Eveleigh, D.; Rowley, B.; Liu, L.; Adnane, L.; Lynch, M.; Auclair, D.; Taylor, I.; Gedrich, R.; Voznesensky, A.; Riedl, B.; Post, L. E.; Bollag, G.; Trail, P. A. *Cancer Res.* **2004**, *64*, 7099.
- (a) Escudier, B.; Eisen, T.; Stadler, W. M.; Szczylik, C.; Oudard, S.; Siebels, M.; Negrier, S.; Chevreau, C.; Solska, E.; Desai, A. A.; Rolland, F.; Demkow, T.; Hutson, T. E.; Gore, M.; Freeman, S.; Schwartz, B.; Shan, M.; Simantov, R.; Bukowski, R. M. N. *Engl. J. Med.* **2007**, *356*, 125; (b) Ryan, C. W.; Goldman, B. H.; Lara, P. N.; Mack, P. C.; Beer, T. M.; Tangen, C. M.; Lemmon, D.; Pan, C. X.; Drabkin, H. A.; Crawford, E. D. J. *Clin. Oncol.* **2007**, *25*, 3296; (c) Abou-Alfa, G. K.; Schwartz, L.; Ricci, S.; Amadori, D.; Santoro, A.; Figer, A.; De Greve, J.; Douillard, J. Y.; Lathia, C.; Schwartz, B.; Taylor, I.; Moscovici, M.; Saltz, L. B. *Clin. Oncol.* **2006**, *24*, 4293; (d) Llovet, J. M.; Ricci, S.; Mazzaferro, V.; Hilgard, P.; Gane, E.; Blanc, J. F.; De Oliveira, A. C.; Santoro, A.; Raoul, J. L.; Forner, A.; Schwartz, M.; Porta, C.; Zeuzem, S.; Bolondi, L.; Greten, T. F.; Galle, P. R.; Seitz, J. F.; Borbath, I.; Häussinger, D.; Giannaris, T.; Shan, M.; Moscovici, M.; Voliotis, D.; Bruix, J. N. *Engl. J. Med.* **2008**, *359*, 378.
- (a) Wong, C. I.; Koh, T. S.; Soo, R.; Hartono, S.; Thng, C. H.; McKeegan, E.; Yong, W. P.; Chen, C. S.; Lee, S. C.; Wong, J.; Lim, R.; Sukri, N.; Lim, S. E.; Ong, A. B.; Steinberg, J.; Gupta, N.; Pradhan, R.; Humerickhouse, R.; Goh, B. C. J. *Clin. Oncol.* **2009**, *27*, 4718; (b) Jain, L.; Woo, S.; Gardner, E. R.; Dahut, W. L.; Kohn, E. C.; Kummur, S.; Mould, D. R.; Giaccone, G.; Yarchoan, R.; Venitz, J.; Figg, W. D. *Br. J. Clin. Pharmacol.* **2011**, *72*, 294.
- (a) Ederhy, S.; Cohen, A.; Dufaitre, G.; Izzedine, H.; Massard, C.; Meuleman, C.; Besse, B.; Berthelot, E.; Boccara, F.; Soria, J. C. *Target Oncol.* **2009**, *4*, 89; (b) ODAC Briefing Document Drug Substance Vandetanib (ZD6474) Date 25 October 2010.
- Melting points were determined in open capillary tubes on a Büchi reference B-530 digital melting point apparatus and are uncorrected. NMR spectra were determined on a Bruker AV-400 (400 MHz) spectrometer in DMSO-*d*<sub>6</sub> or in CDCl<sub>3</sub> at ambient temperature. Low resolution mass spectral (MS) data were determined on an Agilent 1100 Series LC-MS with UV detection at 254 nm and a low resonance electrospray mode (ESI). Chemical shifts are reported in ppm from the solvent resonance (DMSO-*d*<sub>6</sub>, 2.49 ppm).  
A typical procedure utilized is demonstrated for compound **1a** as a representative example. A mixture of 4-chloro-7-piperidinemethoxyquinazoline 100.0 mg (0.344 mmol), **11a** 112.8 mg (0.344 mmol), and isopropanol (15 mL) was stirred at 85 °C for 2 h. The mixture was concentrated under reduced pressure, diluted with AcOEt and washed with water, brine, dried over anhydrous magnesium sulfate, and concentrated under reduced pressure. The residue was purified by basic silica gel column chromatography to afford of **1a** (186.5 mg, yield 93.0%). Compound **1a**: <sup>1</sup>H NMR (400 MHz, DMSO-*d*<sub>6</sub>):  $\delta$  1.67–1.76 (m, 2H), 1.95–2.08 (m, 3H), 2.67–2.68 (m, 3H), 2.97–3.00 (m, 2H), 3.17 (s, 1H), 3.38–3.41 (m, 2H), 3.73–3.79 (m, 2H), 4.05–4.07 (m, 2H), 7.41–7.48 (m, 4H), 7.61–7.66 (m, 2H), 7.94–8.00 (m, 1H), 8.30–8.34 (m, 1H), 8.77 (s, 1H), 9.05–9.07 (m, 1H), 11.42–11.50 (m, 1H), 11.85 (s, 1H). LC-MS (APCI+): *m/z* 583 (MH+).  
Compound **1b**: <sup>1</sup>H NMR (400 MHz, DMSO-*d*<sub>6</sub>):  $\delta$  1.32–1.35 (m, 2H), 1.74–1.77 (m, 3H), 1.83–1.88 (m, 2H), 2.15 (s, 3H), 2.76–2.79 (m, 2H), 3.66 (s, 2H), 3.98–4.00 (m, 2H), 4.30–4.33 (m, 1H), 7.13–7.14 (m, 1H), 7.20–7.23 (m, 1H), 7.30–7.32 (m, 2H), 7.64–7.66 (m, 1H), 7.75–7.77 (m, 2H), 7.83–7.86 (m, 1H), 8.19–8.20 (m, 1H), 8.42–8.47 (m, 2H), 9.62 (s, 1H), 10.58 (s, 1H). LC-MS (APCI+): *m/z* 499 (MH+).  
Compound **1c**: <sup>1</sup>H NMR (400 MHz, DMSO-*d*<sub>6</sub>):  $\delta$  1.32–1.39 (m, 2H), 1.69–1.77 (m, 4H), 1.86–1.91 (m, 2H), 2.16 (s, 3H), 2.78–2.81 (m, 2H), 3.62 (s, 2H), 3.98–4.00 (m, 2H), 7.13–7.23 (m, 2H), 7.30–7.38 (m, 3H), 7.74–7.81 (m, 1H), 8.42–8.47 (m, 2H), 9.61 (s, 1H), 10.37 (s, 1H). LC-MS (APCI+): *m/z* 517 (MH+).  
Compound **1d**: <sup>1</sup>H NMR (400 MHz, DMSO-*d*<sub>6</sub>):  $\delta$  1.15–1.20 (m, 2H), 1.22–1.39 (m, 4H), 1.70–1.76 (m, 4H), 1.85–1.90 (m, 1H), 2.16 (s, 3H), 2.78–2.80 (m, 2H), 3.20 (t, 2H), 6.54–6.58 (m, 2H), 7.07 (s, 1H), 7.13–7.22 (m, 2H), 7.30–7.33 (m,

2H), 8.24–8.35 (m, 2H), 9.33 (s, 1H). LC-MS (APCI+): *m/z* 435 (MH+).

Compound **1e**: <sup>1</sup>H NMR (400 MHz, DMSO-*d*<sub>6</sub>): δ 1.22–1.39 (m, 4H), 1.71–1.77 (m, 4H), 1.85–1.90 (m, 1H), 2.16 (s, 3H), 2.78–2.80 (m, 4H), 3.95 (s, 1H), 3.98–4.00 (m, 2H), 4.94 (s, 1H), 6.54–6.58 (m, 2H), 7.07 (s, 1H), 7.13–7.22 (m, 2H), 7.30–7.33 (m, 2H), 8.24–8.35 (m, 2H), 9.33 (s, 1H). LC-MS (APCI+): *m/z* 446 (MH+).

Compound **1f**: <sup>1</sup>H NMR (400 MHz, DMSO-*d*<sub>6</sub>): δ 1.14–1.91 (m, 15H), 2.16 (s, 3H), 2.72–2.87 (m, 5H), 3.97–3.99 (m, 2H), 6.01–6.03 (m, 1H), 7.10–7.11 (m, 1H), 7.17–7.20 (m, 1H), 7.34–7.36 (m, 2H), 7.59–7.61 (m, 2H), 8.25 (s, 1H), 8.38–8.42 (m, 2H), 9.51 (s, 1H). LC-MS (APCI+): *m/z* 488 (MH+).

Compound **1g**: <sup>1</sup>H NMR (400 MHz, DMSO-*d*<sub>6</sub>): δ 1.32–1.38 (m, 2H), 1.74–1.89 (m, 5H), 2.15 (s, 3H), 2.77–2.79 (m, 2H), 7.12 (s, 1H), 7.19–7.22 (m, 1H), 7.46–7.48 (2H), 7.57–7.71 (m, 4H), 8.13–8.14 (m, 1H), 8.40–8.45 (m, 2H), 9.35 (s, 1H), 9.57 (s, 1H), 9.71 (s, 1H). LC-MS (APCI+): *m/z* 584 (MH+).

Compound **1h**: <sup>1</sup>H NMR (400 MHz, DMSO-*d*<sub>6</sub>): δ 1.30–1.38 (m, 2H), 1.75–1.77 (m, 3H), 1.86–1.97 (m, 2H), 2.16 (s, 3H), 2.78–2.81 (m, 2H), 3.98–4.00 (m, 2H), 6.74–6.78 (m, 1H), 7.05–7.51 (m, 7H), 7.64–7.71 (m, 2H), 8.40–8.45 (m, 2H), 8.71 (s, 1H), 8.88 (s, 1H), 9.57 (s, 1H). LC-MS (APCI+): *m/z* 500 (MH+).

Compound **1i**: <sup>1</sup>H NMR (400 MHz, DMSO-*d*<sub>6</sub>): δ 1.33–1.36 (m, 2H), 1.75–1.77 (m, 3H), 1.84–1.90 (m, 2H), 2.15 (s, 3H), 2.77–2.80 (m, 2H), 3.98–4.00 (m, 2H), 7.10–7.12 (m, 2H), 7.19–7.22 (m, 1H), 7.29–7.36 (m, 1H), 7.42–7.45 (m, 2H), 7.63–7.71 (m, 3H), 8.40–8.45 (m, 2H), 8.70 (s, 1H), 8.85 (s, 1H), 9.57 (s, 1H). LC-MS (APCI+): *m/z* 518 (MH+).

Compound **1j**: <sup>1</sup>H NMR (400 MHz, DMSO-*d*<sub>6</sub>): δ 1.30–1.39 (m, 2H), 1.74–1.77 (m, 3H), 1.85–1.90 (m, 1H), 2.16 (s, 3H), 2.27 (s, 3H), 2.77–2.80 (m, 2H), 3.94 (s, 1H), 3.97–3.99 (m, 2H), 7.06–7.66 (m, 8H), 7.81 (s, 1H), 8.38 (s, 1H), 8.55 (d, 1H), 9.38 (s, 1H). LC-MS (APCI+): *m/z* 605 (MH+).

Compound **1k**: <sup>1</sup>H NMR (400 MHz, DMSO-*d*<sub>6</sub>): δ 1.70–1.73 (m, 2H), 1.85–1.90 (m, 2H), 2.36 (s, 3H), 2.78–2.80 (m, 4H), 3.98–4.00 (m, 1H), 6.54–6.58 (m, 2H), 7.13–7.22 (m, 2H), 7.30–7.33 (m, 5H), 8.24–8.35 (m, 2H), 9.53 (s, 1H), 10.33 (s, 1H). LC-MS (APCI+): *m/z* 579 (MH+).

Compound **1l**: <sup>1</sup>H NMR (400 MHz, DMSO-*d*<sub>6</sub>): δ 1.64–1.71 (m, 2H), 1.97–2.00 (m, 2H), 2.70–2.71 (m, 3H), 2.93–3.60 (m, 4H), 4.08–4.27 (m, 1H), 6.76–6.81 (m, 1H), 7.12–8.19 (m, 9H), 8.71–8.99 (m, 2H), 9.87–9.94 (m, 1H), 10.52 (s, 1H). LC-MS (APCI+): *m/z* 518 (MH+).

Compound **1m**: <sup>1</sup>H NMR (400 MHz, DMSO-*d*<sub>6</sub>): δ 1.45–1.48 (m, 2H), 1.86–1.89 (m, 3H), 2.43 (s, 3H), 2.49 (s, 2H), 3.08 (s, 2H), 4.03–4.04 (m, 2H), 6.77–6.81 (m, 1H), 7.10–7.12 (m, 1H), 7.18 (s, 1H), 7.23–7.34 (m, 2H), 7.49–7.52 (m, 1H), 7.72–7.74 (m, 1H), 8.04–8.06 (m, 1H), 8.13–8.14 (m, 1H), 8.36 (s, 1H), 8.44–8.46 (m, 1H), 8.55 (s, 1H), 9.63 (s, 1H), 9.70 (s, 1H). LC-MS (APCI+): *m/z* 534 (MH+).

Compound **1n**: <sup>1</sup>H NMR (400 MHz, DMSO-*d*<sub>6</sub>): δ 1.60–1.69 (m, 2H), 1.85–1.99

(m, 2H), 2.10 (m, 1H), 2.72 (s, 1H), 2.97–3.03 (m, 2H), 3.45 (m, 2H), 4.00–4.23 (m, 5H), 4.94 (s, 1H), 6.73–6.77 (m, 1H), 7.10–7.12 (m, 1H), 7.28–7.60 (m, 7H), 8.30 (s, 1H), 8.76 (s, 1H), 9.59 (s, 1H), 9.70 (s, 1H), 11.37 (s, 1H). LC-MS (APCI+): *m/z* 531 (MH+).

Compound **1o**: <sup>1</sup>H NMR (400 MHz, DMSO-*d*<sub>6</sub>): δ 1.60–1.69 (m, 2H), 1.97–2.02 (m, 2H), 2.12 (m, 1H), 2.73 (s, 3H), 2.94–3.03 (m, 1H), 4.03 (s, 1H), 4.05–4.07 (m, 2H), 6.76–6.78 (m, 1H), 7.11–7.13 (m, 1H), 7.28–7.52 (m, 4H), 7.75–7.7 (m, 4H), 8.14–8.19 (m, 1H), 8.37 (s, 1H), 8.84 (s, 1H), 8.92 (s, 1H), 9.81 (s, 1H), 11.47 (s, 1H). LC-MS (APCI+): *m/z* 549 (MH+).

- HTRF assays are homogeneous time-resolved assays that generate a signal by FRET between donor and acceptor molecules. When formatted for kinase assays, the Eu-cryptate is usually conjugated to a phospho-specific antibody and is presented upon binding of the antibody to the phosphorylated product, while the streptavidin-conjugated allophycocyanin binds to the biotin on the substrate to complete the detection complex. When the two entities get close proximity and upon excitation, energy transfer occurs and APC emits a specific long-lived fluorescence at 665 nm. The kinases were purified as the intracellular domain of human VEGFR-2 fused by GST. The catalytic activity of the kinase was detected by using a biotinylated synthetic peptide as a substrate, biotin-aminohexyl-EEEEYFELVAKKKK-NH<sub>2</sub>, for VEGFR-2. Phosphorylated substrate is measured by streptavidin linked-APC and europium-labeled anti-phosphorylated tyrosine antibody. In briefly the assay method as follow: the working solution (100 nM TK-substrate, 3 μg/ml GST-VEGFR-2, 100 nM ATP, 1 mM DTT, 1 mM MnCl<sub>2</sub>, 5 mM MgCl<sub>2</sub> and 20 nM SEB in 10 μl reaction volume) incubated at 37 °C for 30 min; the detection solution (6.25 nM Streptavidin-XL665, 5 μl/well TK antibody-cryptate) was added to stop reaction, and placed at room temperature for 30 min for determination (excitation at 314 nm, emission at 665 nm/emission at 620 nm).
- Cell assay: HUVEC were grown in M199 containing 10% FBS and kanamycin (50 U ml<sup>-1</sup>) in a humidified 5% CO<sub>2</sub> incubator at 37 °C. After the cells had grown to confluence, they were disaggregated in trypsin solution, washed with M199 containing 10% FBS, centrifuged at 125 g for 5 min, re-suspended, and then subcultured according to standard protocols. Cells from passages 4–8 were used. HUVEC proliferation in the presence of growth factors was evaluated using Sulforhodamine B (SRB) assay. Briefly, HUVECs were plated in 96-well plates (1000 cells/well) and dosed with tested compound +VEGF (15 ng/ml). The cultures were incubated for 48 h (37 °C; 5% CO<sub>2</sub>) and then plated with SRB and reincubated for 15 min. Cells were harvested and assayed using a ELISA counter to read at 490 nm. IC<sub>50</sub> data were interpolated as described above.